Simulations on Radiative Condensation in Solar Corona

Chun Xia, Rony Keppens, Oliver Porth

Centre for mathematical Plasma Astrophysics, KU Leuven

Juelich, Sept 14, 2015

Outline

Prominences

$6000 \sim 8000$ K $\quad 10^{10} \sim 10^{11}$ cm^{-3}

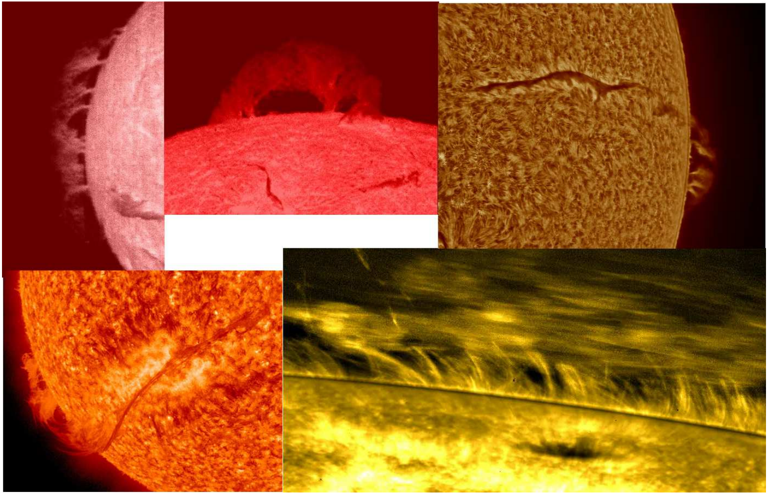

Filaments

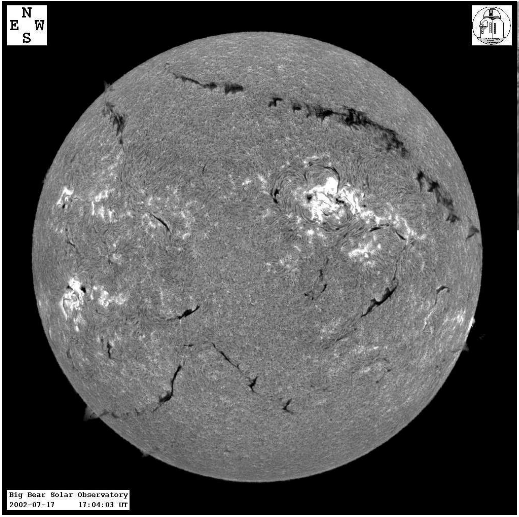

N
E
W
S
Big Bear Solar Observatory
2002-07-17 17:04:03 UT

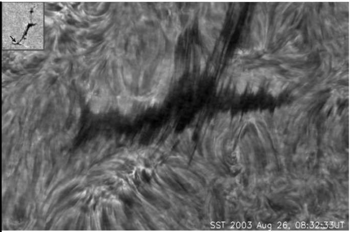

SST 2003 Aug 26, 08:32:33UT

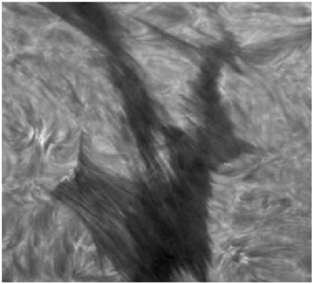

Prominence and coronal cavity

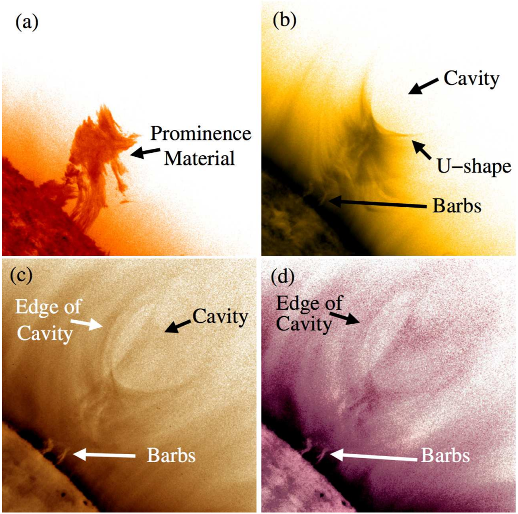

SDO/AIA EUV images
(a) 304 Å 80,000 K
(b) 171 Å 800,000 K
(c) 193 Å 1.5 MK
(d) 211 Å 1.8 MK
(Regnier et al. 2011, A&A)

Prominence and coronal cavity

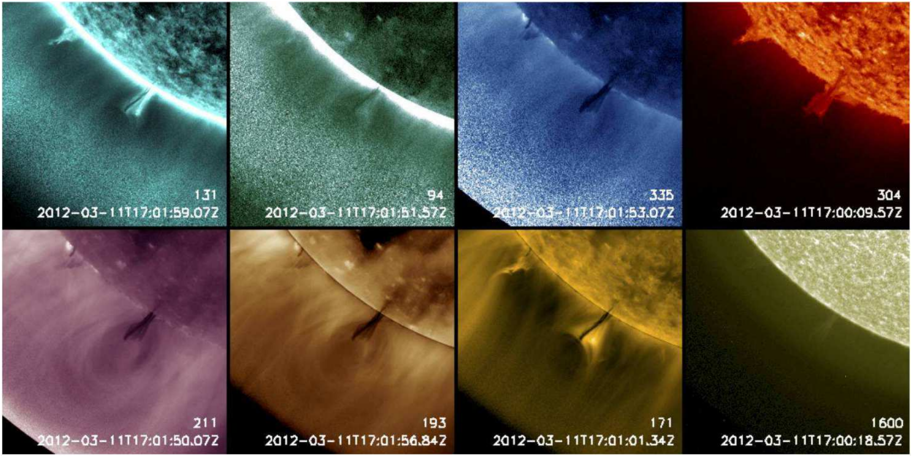

(Su et al. 2015, ApJ)

Prominence, cavity, and streamer

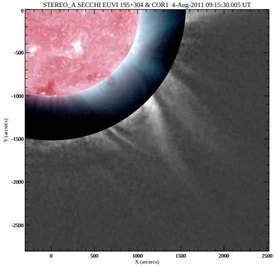

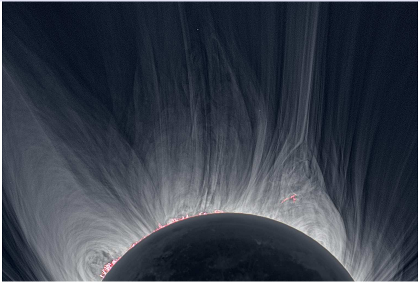

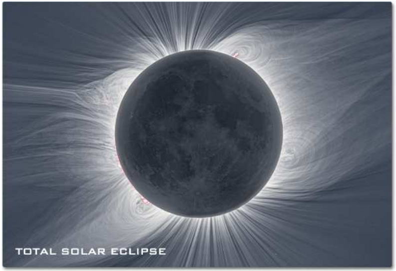

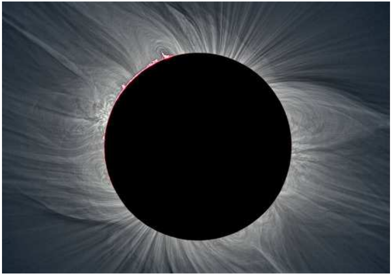

Observations of in situ condensation in a cavity

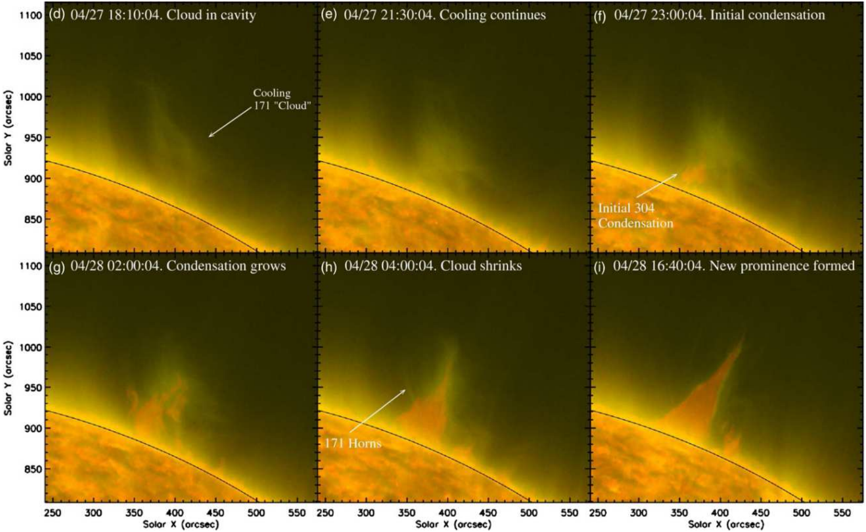

(Berger et al. 2012, ApJL)

Observations of in situ condensation in a cavity

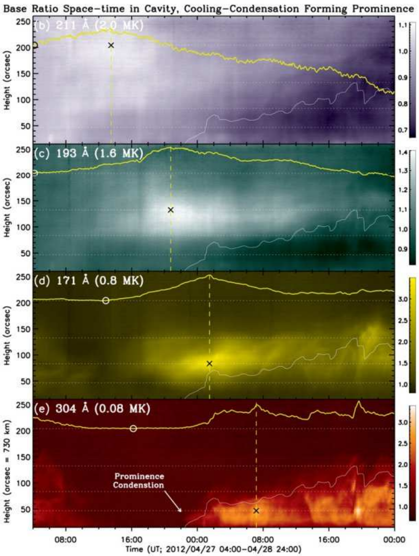

Morphological sketch of prominence and cavity

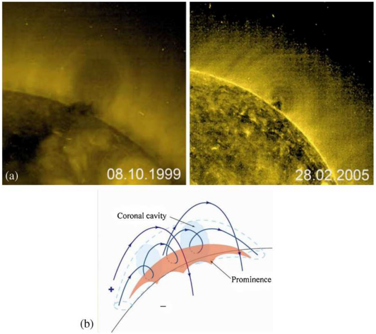

Figure 2. Coronal cavities observed in the SOHO EIT Fe XV 284 Å images (**a**) and a scheme of a coronal flux rope (**b**) (courtesy: SOHO/EIT Consortium).

A helical magnetic flux rope hosts a tunnel-like cavity with a prominence in the lower part. (Boris Filippov et al. 2015, JAA)

Outline

Magnetostatic models

- K–S models for normal polarity prominences (Kippenhahn & Schüter 1957, Anzer 1972, Malherbe & Priest 1983)

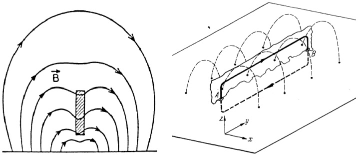

- K–R models for inverse polarity prominences (Kuperus & Raadu 1974, Aner & Priest 1985, Low & Hundhausen 1995)

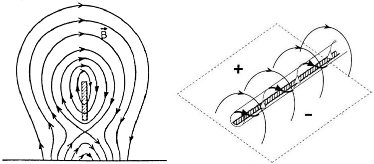

MHD models: birth of a flux rope

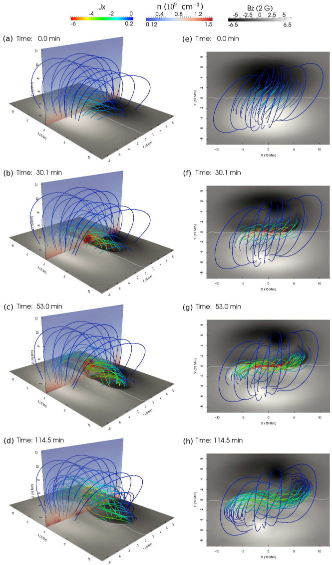

Birth of a flux rope in 1 MK corona caused by systematic converging flows at the bottom formation

- converging flows bring feet of inner loops together
- head-to-tail connection of loops at their feet => helical field lines
- new helical field lines wrap around older ones => a large scale helical flux rope
- The flux rope rises, expands, and relaxes => stable state

(Xia et al. 2014, ApJ)

Outline

Thermal instability theory in uniform plasma

heat-loss function $L = R - H - \kappa\nabla^2 T$: the energy losses minus the energy gains per unit volume per second

$$Ldt = -TdS$$

$$\delta Ldt = -Td(\delta S), \quad \delta L = \left(\frac{\partial L}{\partial S}\right)_A \delta S$$

$$\frac{1}{\delta S}\frac{d(\delta S)}{dt} = -\frac{1}{T}\left(\frac{\partial L}{\partial S}\right)_A$$

$$\delta S = S_0 exp(\int -\frac{1}{T}\left(\frac{\partial L}{\partial S}\right)_A dt), \left(\frac{\partial L}{\partial S}\right)_A < 0$$

Isochoric Criterion ($A = \rho$):

$$\left(\frac{\partial L}{\partial S}\right)_\rho = \left(\frac{\partial L}{\partial T}\right)_\rho \left(\frac{\partial T}{\partial S}\right)_\rho = \left(\frac{\partial L}{\partial T}\right)_\rho \frac{T}{C_v} < 0$$

$$TdS = C_v dT, \left(\frac{\partial L}{\partial T}\right)_\rho < 0$$

$$T = T_0 + T_1, \; T_1 = A\sin(kx)e^{ct}, \; \kappa\nabla^2 T = -\kappa k^2 T_1$$

$$\left(\frac{\partial (R-H)}{\partial T}\right)_\rho + \kappa k^2 < 0$$

Isobaric Criterion ($A = p$):

$$\left(\frac{\partial L}{\partial S}\right)_p = \left(\frac{\partial L}{\partial T}\right)_p \left(\frac{\partial T}{\partial S}\right)_p = \left(\frac{\partial L}{\partial T}\right)_p \frac{T}{C_p} < 0$$

$$TdS = C_p dT, \left(\frac{\partial L}{\partial T}\right)_p < 0$$

$$\left(\frac{\partial L}{\partial T}\right)_p = \left(\frac{\partial L}{\partial T}\right)_\rho + \left(\frac{\partial L}{\partial \rho}\right)_T \left(\frac{\partial \rho}{\partial T}\right)_p$$

$$= \left(\frac{\partial L}{\partial T}\right)_\rho - \left(\frac{\partial L}{\partial \rho}\right)_T \frac{\rho}{T} < 0$$

$$\left(\frac{\partial (R-H)}{\partial T}\right)_\rho + \kappa k^2 - \left(\frac{\partial (R-H)}{\partial \rho}\right)_T \frac{\rho}{T} < 0$$

$R \propto \rho^2 T^{-1}, \; T \in 1 \sim 2$ MK

1D HD models

- 1D hydrodynamic simulations along individual magnetic loop
- localized heating near loop feet => chromospheric evaporation
- strong radiation $R = n^2\Lambda(T)$=> thermal non-equilibrium => catastrophic cooling => condensation

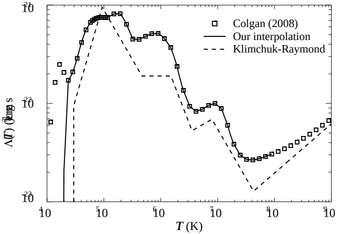

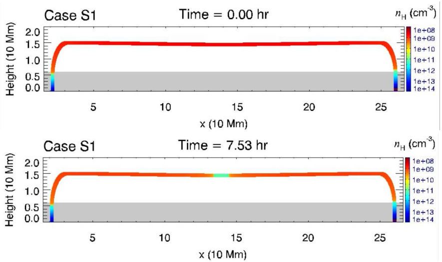

(Antiochos et al. 1999; Karpen et al. 2001, 2005, 2008; Xia et al. 2011).

1D Evaporation-condensation model

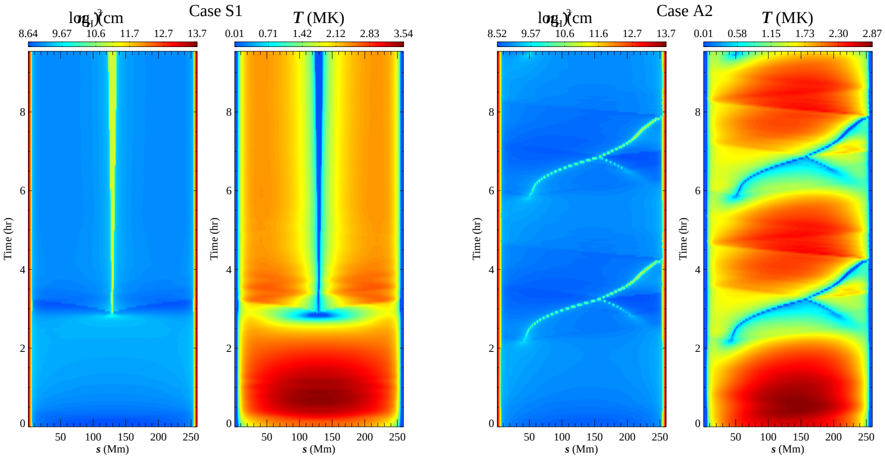

(Xia et al. 2011)

Evidence of thermal instability

Evolution of loop center in case S1

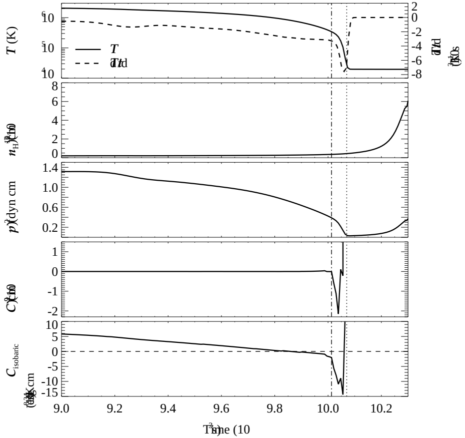

- isochoric criterion (Parker 1953)

$$\left(\frac{\partial(R-H)}{\partial T}\right)_\rho + \kappa k^2 < 0$$

- isobaric criterion (Field 1965)

$$\left(\frac{\partial(R-H)}{\partial T}\right)_\rho + \kappa k^2 - \left(\frac{\partial(R-H)}{\partial \rho}\right)_T \frac{\rho}{T} < 0$$

- Both criteria turn to significantly negative when catastrophic cooling

3D views of multiple 1D model assembly

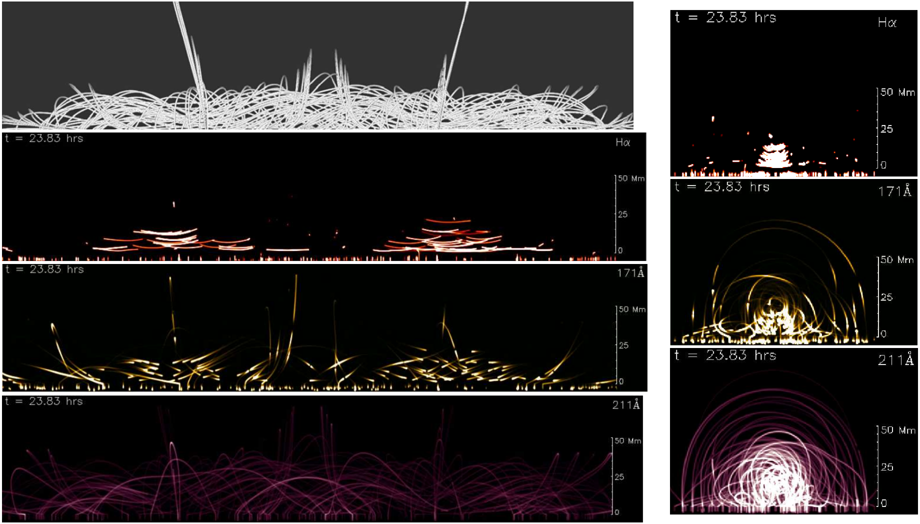

(Luna et al. 2012, ApJ)

2.5D prominence formation (1/2) (Xia et al. 2012, ApJ)

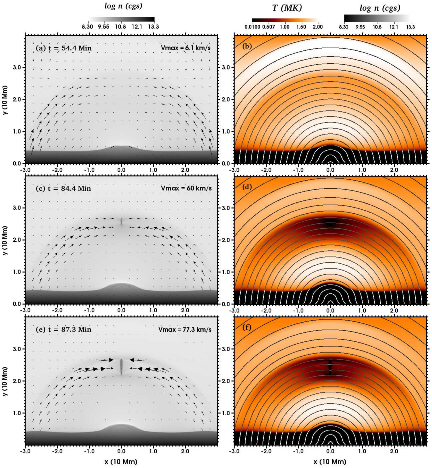

localized heating concentrated at strong B_y regions:
First condensation: Time=84 Min, Height=25.4 Mm, Shear Angle=28°
Shocks are launched and damped quickly. forced left-right symmetry by only simulating the right half.

Thermal Instability

Evolution at the first condensation site

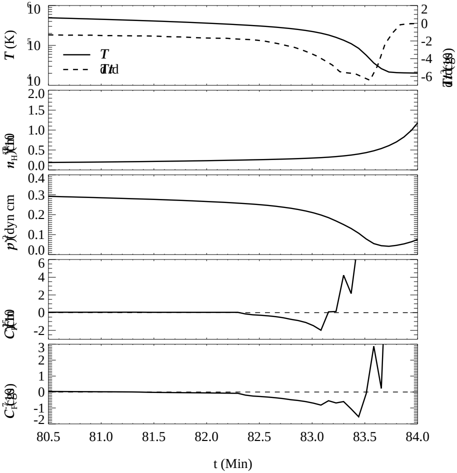

- isochoric thermal instability criterion C_P, isobaric criterion C_F
- Both criteria turn to significantly negative when catastrophic cooling.

Adaptive Refined Grids

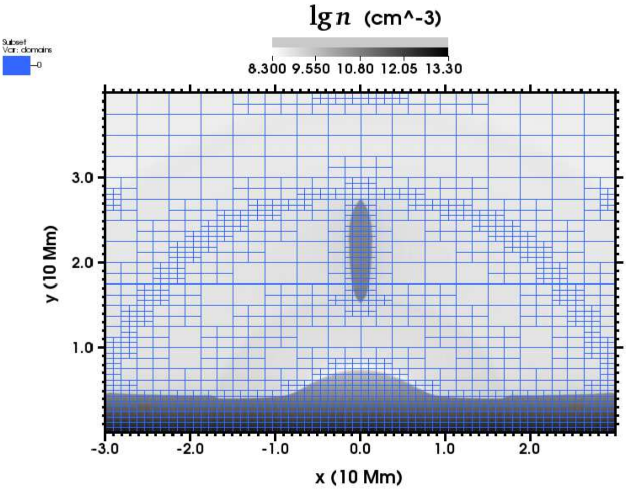

2.5D prominence formation (2/2) (Keppens and Xia 2014, ApJ)

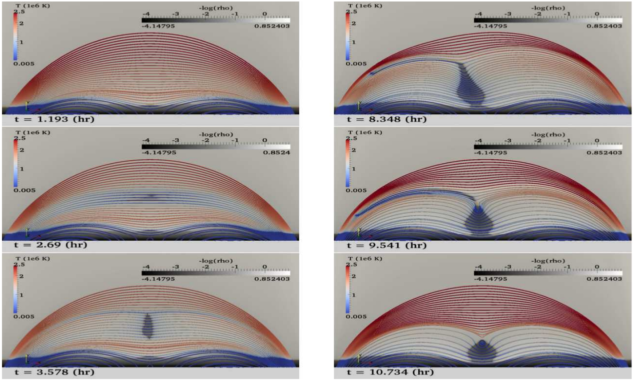

coronal condensation in magnetic dips of 2.5D arcade, asymmetric dynamics develop (coronal rain, flux rope)

3D prominence formation (Xia et al. 2014, ApJL)

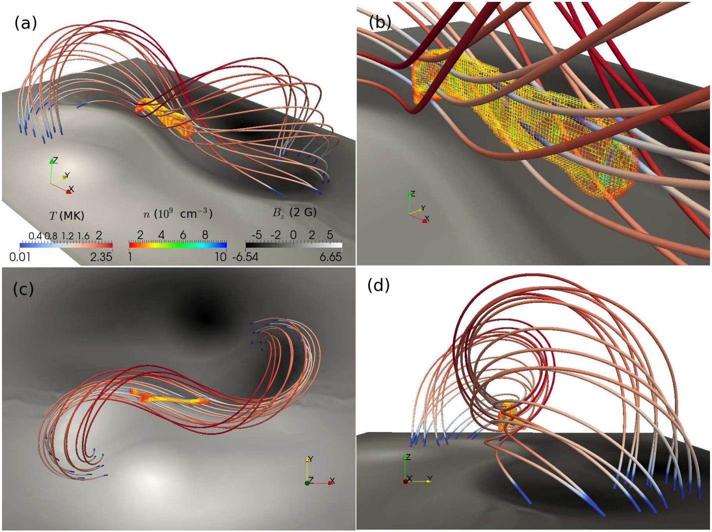

Dynamic condensation in AIA synthetic views

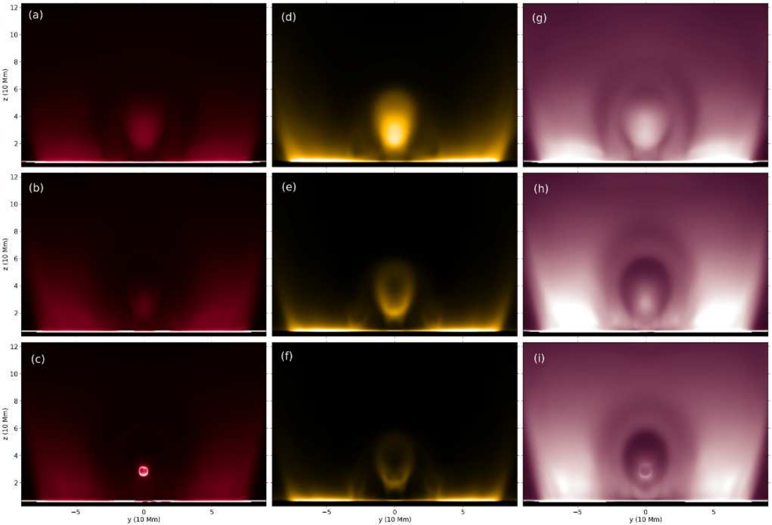

AIA synthetic views of the prominence and cavity

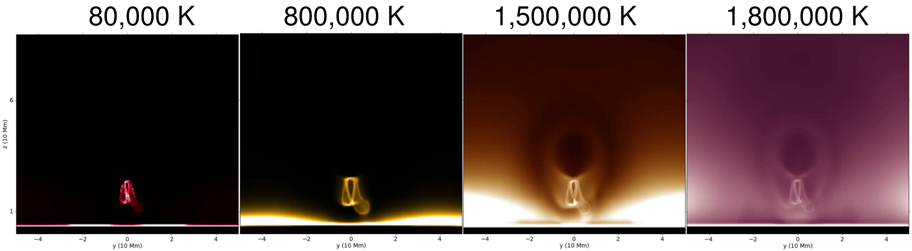

- Protruding tail ('barb') extends to lower altitude
- "horns" extend from the top of the prominence to the upper cavity in 193 and 211 bands
- density depletion in the cavity (20 $\sim$ 30 %), 2 MK temperature

Outline

Model initial setup

- Use Cartesian 3D box, horizontal axes x (-100,100) Mm and y (-60,60) Mm, vertical axis z (0, 80) Mm
- isothermal MHD with constant temperature $T_0 = 1$ MK and gravity, no energy equation

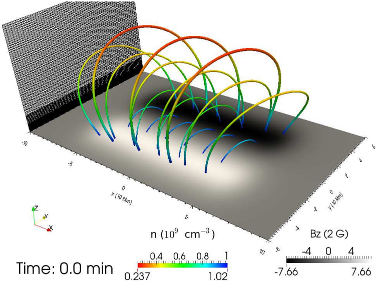

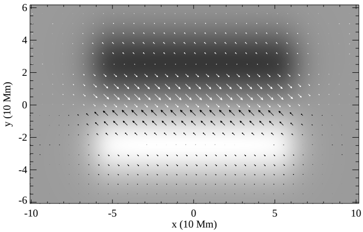

Numerical methods and boundary conditions

- code: isothermal MHD solver of MPI-AMRVAC (Porth et al 2014, ApJS)
- scheme: HLL and Cada slope limiter, three-step Runge–Kutta
- mesh: 3-level AMR, resolution: $400 \times 240 \times 240$, 333 km per cell
- boundary conditions:
  velocity: shearing and converging horizontal flows at the bottom; zero velocity at other boundaries
  magnetic field: zero gradient extrapolation and modified normal field ensuring divergence free at the bottom; fixed at others.
  density: continuous at side boundaries, fixed at the bottom, gravitational hydrostatic stratification at the top
- GLM-MHD method to maintain divergence free of magnetic field (Dedner et al. 2002, JCP)

time series of flux rope formation

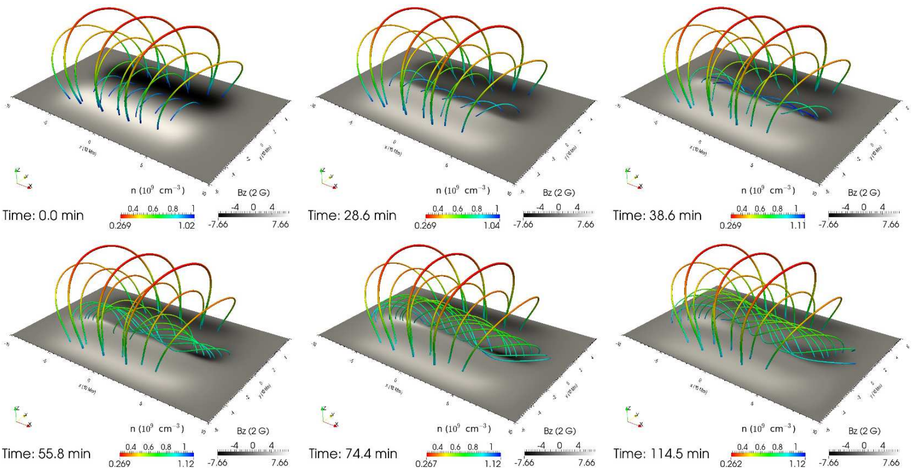

Outline

Initial state

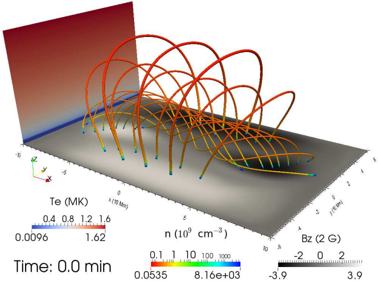

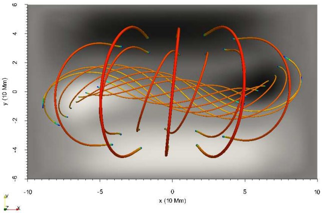

- restart from the isothermal flux rope and add energy equation
- rewrite pressure $p(z)$ and density $\rho(z)$ according to hydrostatic stratification from chromosphere (9600 K, 10^{13} cm^{-3}) to corona (1 $\sim$ 1.6 MK)
- nearly force-balance and thermal non-equilibrium

Assumptions and equations

- MHD equations where $p_{\rm tot} \equiv p + B^2/2$, $p = 2.3 n_{\rm H} k_{\rm B} T$, $\rho = 1.4 m_{\rm H} n_{\rm H}$, $E = p/(\gamma - 1) + \rho v^2/2 + B^2/2\mu_0$:

$$\frac{\partial \rho}{\partial t} + \nabla \cdot (\rho \mathbf{v}) = 0$$

$$\frac{\partial (\rho \mathbf{v})}{\partial t} + \nabla \cdot \left(\rho \mathbf{v}\mathbf{v} + p_{\rm tot} \mathbf{I} - \frac{\mathbf{B}\mathbf{B}}{\mu_0} \right) = \rho \mathbf{g}$$

$$\frac{\partial E}{\partial t} + \nabla \cdot \left(E\mathbf{v} + p_{\rm tot}\mathbf{v} - \frac{\mathbf{B}\mathbf{B}}{\mu_0} \cdot \mathbf{v} \right) = \rho \mathbf{g} \cdot \mathbf{v} + H - R + \nabla \cdot (\boldsymbol{\kappa} \cdot \nabla T)$$

$$\frac{\partial \mathbf{B}}{\partial t} + \nabla \cdot (\mathbf{v}\mathbf{B} - \mathbf{B}\mathbf{v}) = 0$$

- The energy equation with parameterized heating, radiative cooling, and field-aligned thermal conduction

Thermal sources and boundary conditions

- MHD solver in MPI-AMRVAC
- mesh: 4-level AMR, resolution: $800 \times 480 \times 480$, 166 km per cell
- explicit central difference scheme to solve field-aligned ($\boldsymbol{\kappa} = \kappa_{\|}\mathbf{e_B e_B}$) thermal conduction separately using RKL2 Super TimeStepping scheme (Meyer et al. 2012, MN)
- optically thin radiative cooling, $R = 1.2 n_{\mathrm{H}}^2 \Lambda(T)$ using an exact integration scheme (Townsend 2009, ApJS)
- background heating $H_0 = c_0 e^{-z/\lambda}$ with $c_0 = 10^{-4}$ erg cm^{-3} s^{-1} and $\lambda = 60$ Mm
- boundary conditions:
  velocity: zero velocity
  magnetic field: fixed at all boundaries
  pressure and density: continuous at side boundaries, fixed at the bottom, gravitational hydrostatic stratification at the top

Relaxing to an equilibrium with background heating

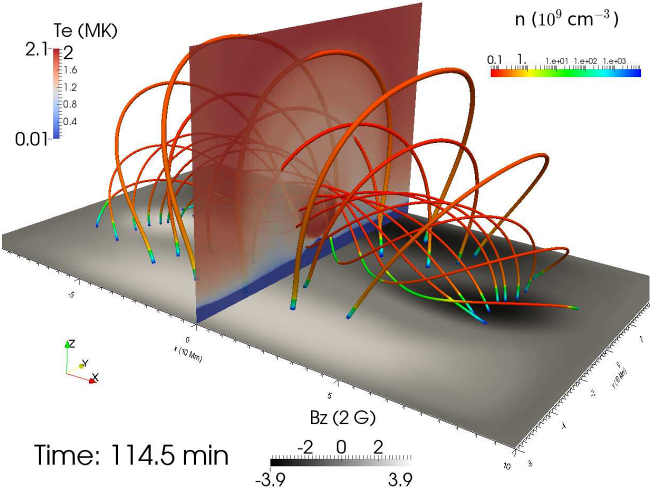

Add localized heating at footpoint regions

$$H_1 = \begin{cases} f(t) c_1 e^{-((z-zh)/H_m)^2} & \text{if } z > zh \\ f(t) c_1 & \text{if } z \leq zh \end{cases} \qquad f(t) = \begin{cases} (t - tr)/tr & \text{if } t \leq tr \\ 1 & \text{if } t > tr \end{cases}$$

where $c_1 = 10^{-2}$ erg cm^{-3} s^{-1}, $zh = 5$ Mm and $H_m = 3.16$ Mm

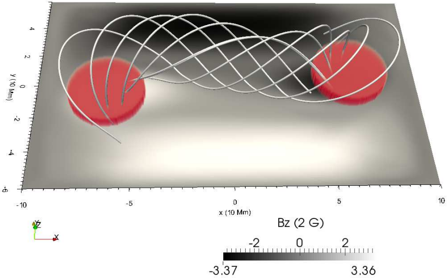

Restart simulation from the equilibrium with total heating $H = H_0 + H_1$

3D condensations in the flux rope

Shown by density contours: yellow 10^{10} cm^{-3}; red 2×10^{10} cm^{-3}

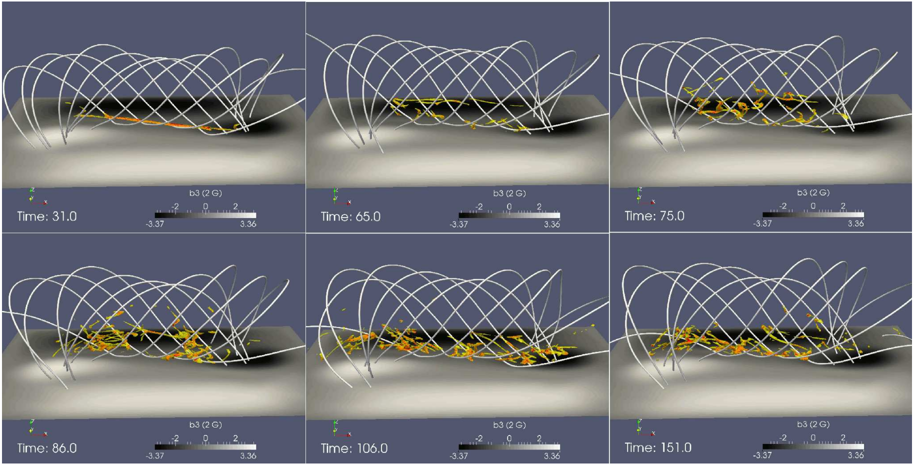

AMR structure in a slice

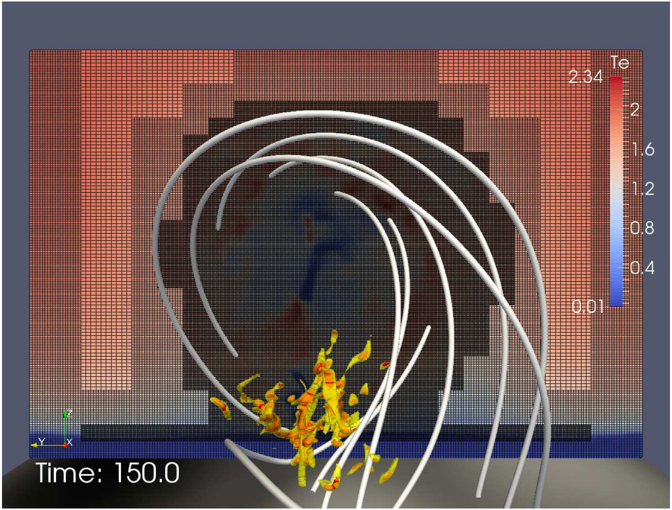

Particle tracers tracking field lines

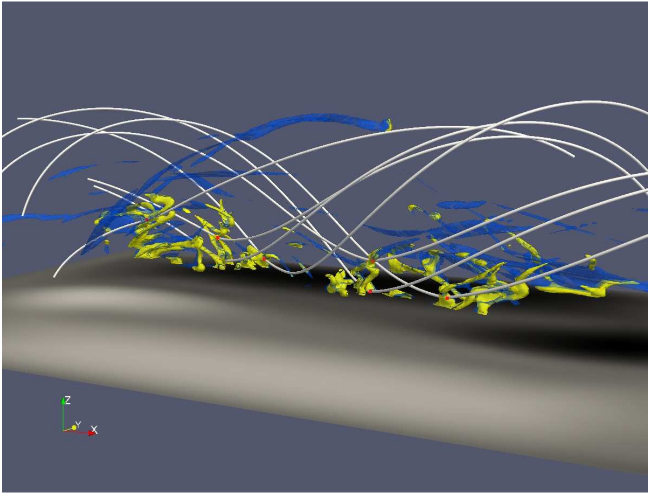

Technique of LOS synthetic view

- Flux of imaging instrument at band i => LOS integral through the plasma

$$F_i = \int n_\mathrm{e}^2 G_i(n_\mathrm{e}, T_\mathrm{e})\, dl \quad [\mathrm{DN\ s}^{-1}], \tag{1}$$

- The instrumental response $G_i(n_\mathrm{e}, T_\mathrm{e})$ => 2D look-up tables using CHIANTI version 7
- LOS integral by interpolation-based ray-tracing with a uniform grid of rays passing through the AMR grid
- typical bands for prominence => EUV wavelength bands 304, 171, 193, and 211 Å SDO/AIA => temperatures 0.08, 0.8, 1.5 up to 1.8 MK, respectively
- emission behind plasma with density higher than 2×10^{10} cm^{-3} is blocked

AIA synthetic views along prominence axis

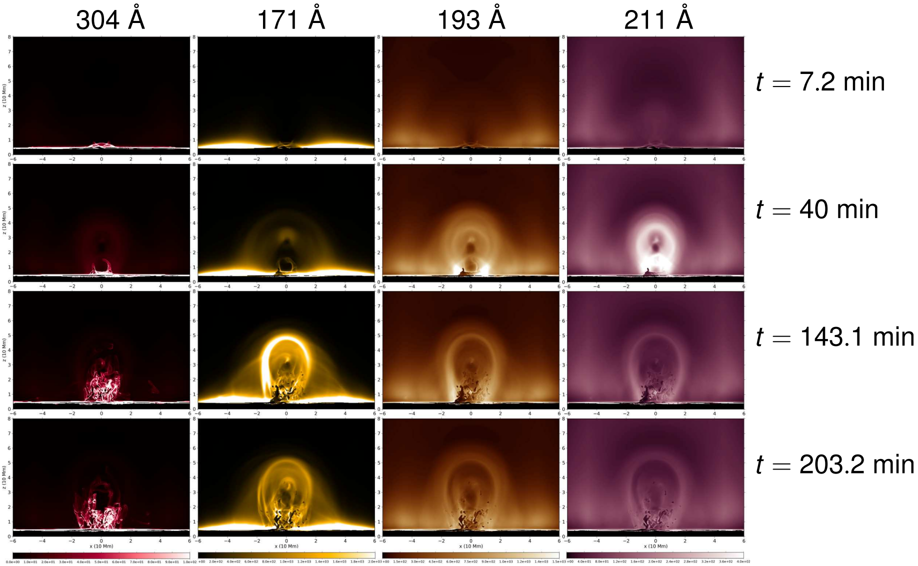

AIA synthetic views on flank of prominence

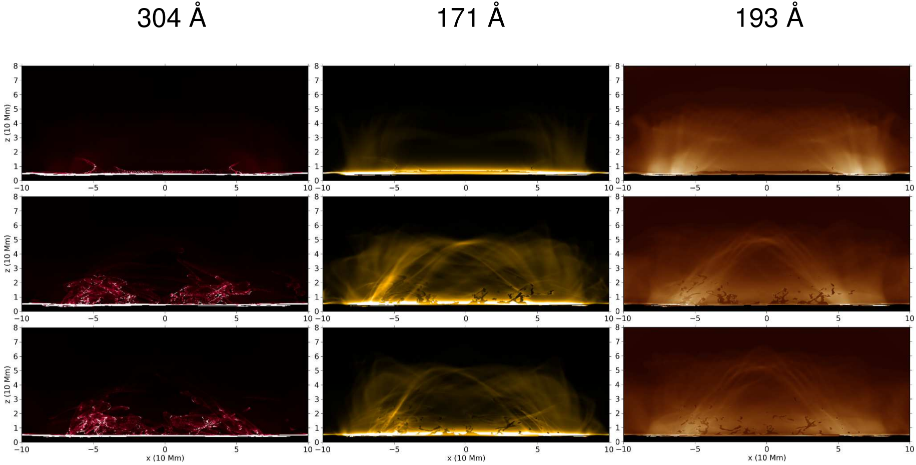

AIA synthetic views from the top

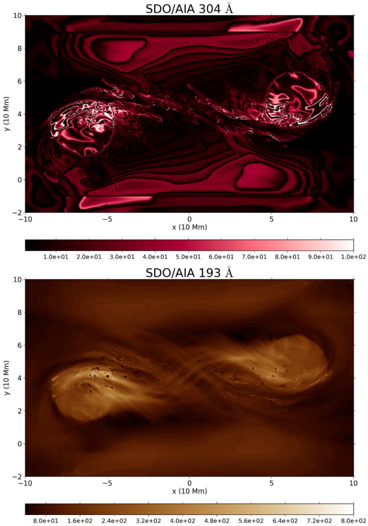

Conclusions

- Thermal instability is responsible for radiative condensation in solar corona.
- Shearing and converging flows at the bottom of corona drive the formation of an elongated magnetic flux rope from an initial sheared arcade.
- Localized heating at two feet of the flux rope evaporates plasma from chromosphere to corona in the flux rope where radiative thermal instability leads to plasma condensations into prominence plasma in shapes of threads and blobs
- prominence mass cycling: chromospheric evaporation => coronal condensation => falling back to chromosphere
- SDO/AIA EUV synthetic axial limb views show the prominence in an elliptical coronal cavity with a core cavity above the prominence